Conformational stability, vibrational assignments, and normal coordinate analysis from FT-IR spectra of xenon solutions and ab initio calculations of epichlorohydrin

ARTICLE *in* JOURNAL OF MOLECULAR STRUCTURE · MARCH 1998

Impact Factor: 1.6 · DOI: 10.1016/S0022-2860(97)00344-X

3 AUTHORS, INCLUDING:

Min-Joo Lee
Changwon National University
23 PUBLICATIONS **166** CITATIONS

SEE PROFILE

ELSEVIER

Journal of Molecular Structure 444 (1998) 99–113

Journal of
MOLECULAR
STRUCTURE

Conformational stability, vibrational assignments, and normal coordinate analysis from FT–IR spectra of xenon solutions and ab initio calculations of epichlorohydrin

Min Joo Lee[a], Seung Won Hur[b], James R. Durig[b,*]

[a]*Department of Chemistry, Changwon National University, Changwon, Kyungnam 641-773, Republic of Korea*
[b]*Department of Chemistry, University of Missouri-Kansas City, Kansas City, MO 64110-2499, USA*

Received 24 July 1997; accepted 1 September 1997

Abstract

Infrared spectra (3500–400 cm^{-1}) of epichlorohydrin (chloromethyloxirane), c-$OC_2H_3C(Cl)H_2$, dissolved in liquid xenon have been recorded at several temperatures from −40 to −105°C. Additionally, the Raman spectrum of the liquid has been obtained from 23 to −39°C. These spectra are consistent with three stable conformers existing in both phases at ambient temperature. The data have been interpreted on the basis that the gauche-2 conformer is the most stable form and the gauche-1 rotamer (most polar) is the second most stable form in the xenon solution whereas the gauche-1 conformer is the most stable form and the cis conformer is the second most stable form in the liquid. Utilizing well separated triplets of three fundamentals due to all three conformers, the enthalpy differences have been determined to be 51 ± 14 cm^{-1} (146 ± 40 cal mol^{-1}) (gauche-2 to gauche-1) and 213 ± 97 cm^{-1} (609 ± 277 cal mol^{-1}) (gauche-2 to cis) in the xenon solution and 383 ± 28 cm^{-1} (gauche-1 to gauche-2) and 358 ± 12 cm^{-1} (gauche-1 to cis) in the liquid. The structural parameters, dipole moments, conformational stability, and vibrational frequencies have been determined by ab initio calculations with two basis sets up to MP2/6-31G*. Vibrational assignments for the 24 normal modes for both the gauche-2 and gauche-1 conformers are proposed with several of the fundamentals assigned for the cis conformer. In addition, some of the fundamental frequencies for motions of the ^{37}Cl isotope have been observed at 2–3 cm^{-1} lower frequency than the corresponding modes of the ^{35}Cl isotope. © 1998 Elsevier Science B.V.

Keywords: Epichlorohydrin; Conformational stability; Ab initio calculations; Infrared spectrum

1. Introduction

The epichlorohydrin (chloromethyloxirane), c-$OC_2H_3C(Cl)H_2$, has been shown to exist as three conformations (Fig. 1) in the fluid phases by ^{13}C NMR [1], microwave [2–4] and vibrational [5] spectroscopies, and electro-optic measurement. [6] The gauche-1 conformer (most polar form) is the only conformer remaining in the solid state. [5,7] However, there are still disagreements on the conformational stability in the fluid phases. In the initial vibrational studies, [7–9] the investigators demonstrated that rotational isomerism was present in the fluid phases and Hayashi et al. [7] concluded that a polar and less polar forms were present in the liquid phase. Charles et al. [10] identified these conformers

* Corresponding author.

PII S0022-2860(97)00344-X

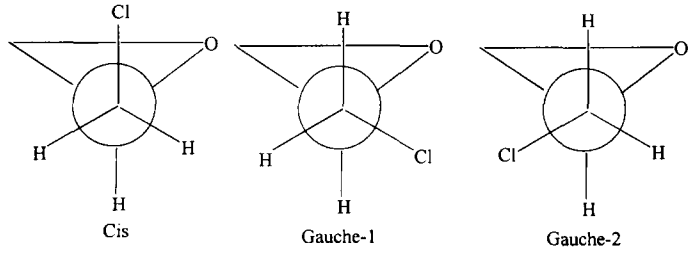

Fig. 1. Newman projections for the three stable conformations of epichlorohydrin.

as the gauche-1 (more polar) and gauche-2 (less polar) forms and determined that ΔH had a value of 1.09 ± 0.20 kcal mol^{-1} in the liquid state with the gauche-1 being the more stable form. However, these authors [10] concluded that the gauche-2 rotamer predominated in the vapor state on the basis that the infrared intensities for the 960/925 cm^{-1} doublet in the liquid sample reversed their intensities (965/934 cm^{-1}) in the spectrum of the vapor. This result was contradicted by another vibrational study [5] where it was concluded that the most stable conformer was the gauche-1 form in both the liquid and vapor phases. More recently, an electron diffraction study [11] reported the gauche-2 as the most stable and the gauche-1 as the second most stable at 67°C and the measurement of the dipole moments and electric birefringences [6] also concluded the gauche-2 form was more abundant (54%) than the other two forms in non-polar solvents.

Therefore, in order to further investigate the relative stability and determine the energy differences among the three conformations of epichlorohydrin, we have carried out studies of the Fourier-transform infrared (FT–IR) spectra of this molecule dissolved in liquid xenon and the Raman spectra of the liquid at variable temperatures. Additionally, theoretical ab initio calculations have also been performed, since our recent studies have shown that the combination of vibrational spectroscopy with ab initio calculations can be a powerful method for understanding conformational behavior of molecules. The ab initio calculations using various basis sets up to the MP2/6-31G* level have been carried out to obtain the optimized structures and vibrational frequencies. We have also utilized the MP2/6-31G* basis set to obtain the force field from which we have performed a normal coordinate analysis for all three conformers. Finally, we have utilized the ab initio predicted energy differences among the conformers to compare with those obtained from experiments. The results of these investigations are reported herein.

2. Experimental

The sample of epichlorohydrin was obtained from Aldrich Chemical Co. (Milwaukee, WI) at a stated purity of 99 + %, and subjected to further purification using a low-temperature, low-pressure fractionation column. After purification, the sample was stored in the dark, and held at 5°C under vacuum in a glass sample tube containing a greaseless stopcock. All subsequent sample manipulations were carried out under vacuum in order to avoid contamination.

The mid-infrared spectrum was recorded on a Bruker model IFS-66 Fourier transform interferometer equipped with a Globar source, Ge/KBr beamsplitter, and a TGS detector. The sample was dissolved in liquified xenon and the spectra were recorded at temperatures ranging from −40 to −105°C. For each temperature investigated, 100 interferograms were collected at a resolution of 1.0 cm^{-1}, averaged, and transformed with a boxcar truncation function. The spectra were obtained with the sample contained in a specially designed cryostat cell which has been described elsewhere [12]. The variable temperature liquid phase Raman spectra were recorded from 23 to −39°C with a Harney–Miller [13] cell, with the sample sealed in a glass capillary. Frequencies obtained from these spectra, in addition to those from the previous study, [5] are compiled in Table 1.

3. Conformational stability

A portion of the infrared spectra (1500–400 cm^{-1}) of the sample in liquid xenon solution at −100°C are

Table 1
Vibrational frequencies (cm^{-1}) and assignments for epichlorohydrin[a]

INFRARED										RAMAN						ASSIGNMENT	
Gas	Rel. Int.	Xe Soln.	Rel. Int.	Liquid*	Rel. Int	Glass*	Rel. Int	Crystal*	Rel. Int	Gas*	Rel. Int	Liquid	Rel. Int	Solid*	Rel. Int	ν_i[b]	Approximate Description
3068 Q																ν_1"	
3063 Q	ms	3054	m							3064	w					ν_1	*CH_2 antisymmetric stretch
3056 Q				3065	m	3072	w	3071	w	3056	vw	3065	mw	3068	w	ν_1'	
3024	m,bd	3015	sh							3024	m					ν_2	CH_2 antisymmetric stretch
												3022	sh	3032	vw	ν_2'	
								3018	sh					3016	m		
		3010	w	3005	s	3011	m	3007	w	3015	m	3006	vs	3005	sh	ν_3'	
3015	m,bd																
		3000	m							3008	mw					ν_3	CH stretch
		2991	sh													ν_3"	
2982 R																	
2975 Q		2963	m							2977	s					ν_4	*CH_2 symmetric stretch
2969 P																	
2963 Q		2953	w	2963	m	2970	mw	2975	w	2965	m	2963	vs	2972	s	ν_4'	
		2927	m							2942	m					ν_5	CH_2 symmetric stretch
2940	w,bd																
		2923	sh	2926	m	2928	w	2928	vw	2936	sh	2926	ms	2926	w	ν_5'	
								2920	sh								
2894 R																ν_{6+8}	
2882 P																	
1496 R	w																
1490 Q		1482	w					1490	w							ν_6	*CH_2 deformation
1487 Q	sh	1480	sh	1480	m	1479	m	1477	w			1478	m	1475	vw	ν_6'	
1483 P																	
1461 R																	
1456 Q	w	1449	m							1456	vw					ν_7	CH_2 deformation
1448 P																	
1439 Q	vw			1446	m	1446	sh					1447	vw			ν_7"	
1437 Q	vw	1431	w	1431	ms	1434	ms	1443	m			1432	w	1442	vw	ν_7'	
1433 P																	
1416 R																	
1412 Q	w	1405	w							1409	m					ν_8	ring breathing
1411 Q	sh															ν_8	^{37}Cl
1408 P																	
1405 Q	sh	1397	w	1403	m	1399	ms	1405	ms			1403	m	1405	m	ν_8'	
														1401	sh		
1402 Q	w	1396	sh	1397	ms					1399	m	1397	ms			ν_8"	
		1292	vw	1298	w											ν_9"	
1280 R																	
1276 Q	ms	1273	s	1275	sh	1280	sh					1276	sh			ν_9	CH_2 rock
1275 Q	sh															ν_9	^{37}Cl
1272 P, R																	
1267 Q	ms	1264	m	1264	vw	1267	s	1270	m,bd	1269	w	1266	m	1266	m	ν_9'	
1263 P																	
1256 Q																ν_{10}"	

Table 1 (*continued*)

INFRARED										RAMAN						ASSIGNMENT	
Gas	Rel. Int.	Xe Soln.	Rel. Int.	Liquid*	Rel. Int	Glass*	Rel. Int	Crystal*	Rel. Int	Gas*	Rel. Int	Liquid	Rel. Int	Solid*	Rel. Int	ν_i[b]	Approximate Description
1256 Q																ν_{10}"	
								1260	s					1258	sh		
1253 Q		1253	w	1254	s	1254	s	1255	s	1253	ms	1253	vs	1254	m	ν_8'	
1246 Q		1243	vw							1244	w					ν_{10}	CH bend
		1240	vw													ν_7-ν_{23}	
		1207	vw	1206	vw	1212	w	1216	w			1208	w	1213	vw	ν_{11}'	
		1202	vw			1196	w					1197	w			ν_{11}"	
1197 R																	
1194 Q	sh	1189	w	1191	w											ν_{11}	CH_2 wag
1192 Q																ν_{11}	^{37}Cl
1186 P																	
1156 R																	
1151 Q	vw	1149	w	1145	sh	1148	sh	1159	w	1150	vw	1148	mw	1160	vw	ν_{12}'	
1144 P																	
1136 Q	sh	1142	vw													ν_{12}	CH bend
1134 Q	vw	1131	w,bd	1134	m	1137	m	1142	w	1134	vw	1134	mw	1139	vw	ν_{13}	*CH_2 wag, g2+g1+*cis*
1098 R																	
1092 Q	vw	1090	w,bd	1090	mw	1094	mw	1091	w	1091	m	1090	m	1091	vw	ν_{14}	CH_2 twist, g2+g1
1087 P														1081	sh		
1073 Q						1073	vw									ν_{14}"	
		1057	vw			1058	vw			1055	vw	1055	vw			ν_{15}'	
		1053	vw													ν_{15}	*CH_2 rock
		1034	vw			1030	vw									ν_{15}"	
972 Q	sh	968	sh													ν_{16}"	
				959	s	961	s			965	w	960	mw				
970 R																	
964 Q	ms	962	s													ν_{16}	C-C stretch
960 P																	
940 R								925	sh					927	sh		
934 Q	w	929	m	924	vs	925	vs	921	s			925	mw	921	w	ν_{16}'	
928 P																	
		911	w	903	m	903	s	908	m			906	mw	910	w	ν_{17}'	
		875	w													ν_{17}	*CH_2 twist
858 R								857	sh					859	w		
853 Q	ms	852	s	850	vvs	852	vvs	848	vs	851	w,bd	853	mw	848	w	ν_{18}'	
846 P																	
842 Q		846	s	840	sh	839	sh			842	mw					ν_{18}	ring symmetric deformation
		838	w													ν_{18}"	
803 R																	
794 P	mw	794	m			786	sh					780	w			ν_{19}	ring antisymmetric deformation
				788	m,bd					790	vw,bd						

Table 1 (*continued*)

INFRARED										RAMAN						ASSIGNMENT	
Gas	Rel. Int.	Xe Soln.	Rel. Int.	Liquid*	Rel. Int	Glass*	Rel. Int	Crystal*	Rel. Int	Gas*	Rel. Int	Liquid	Rel. Int	Solid*	Rel. Int	ν_i[b]	Approximate Description
788	sh	788	w			777	m					773	w			ν_{19}"	
781 R																	
775 Q	mw	769	s	756	s	754	s	754	s			759	m	760	s	ν_{19}'	
														755	sh		
761 R																	
756 Q	vs	750	vs	733	sh	732	sh			755	vs	735	sh			ν_{20}	C-Cl stretch
755 Q	sh																
752 Q	sh	746	sh													ν_{20}	^{37}Cl
749 P																	
								718	sh								
743 Q	m	736	m	720	vvs	715	vvs	713	s	742	ms	721	vs	717	vs	ν_{20}'	
		733	w													ν_{20}'	^{37}Cl
		703	vw	692	mw	690	mw					695	mw			ν_{20}"	
		701	vw													ν_{20}"	^{37}Cl
526 R																	
521 Q		520	vw	516	m	518	mw			520	vw	517	w			ν_{21}"	
518 Q																ν_{21}"	^{37}Cl
511 P																	
443 R																	
438 Q		438	m	441	s	446	vs	453	s	443	w	443	mw	452	sh	ν_{21}'	
430 P														446	w		
		405	vw			413				406	w	413	w			ν_{21}	ring-C(Cl)H_2 out-of-plane bend
						365		374	w	371	s	372	ms	380	s	ν_{22}	ring-C(Cl)H_2 in-plane bend, g2+g1
														373	sh		
218 R																	
214 Q	w					230				211	m	221	w			ν_{23}	CCCl bend
206 P																	
						228										ν_{23}'	
~90	w,bd									86	vw					ν_{24}	C(Cl)H_2 asymmetric torsion
														68	w		lattice mode

[a]Abbreviations used: s, strong, m, moderate; w, weak; v, very; bd, broad; sh, shoulder; A, B, and C refer to infrared band envelopes; P, Q, and R refer to portions of the IR band contours.
*Taken from Ref. 4.
†Denotations used are: ν, fundamental for *gauche*-2 conformer; ν', fundamental for *gauche*-1 conformer; ν", fundamental for *cis* conformer; ^{37}Cl, fundamental of epichlorohydrin of ^{37}Cl isotope.

shown in Fig. 2. From the comparison of these spectra with the previous [5] vibrational spectra and calculated frequencies, several conformational triplets have been identified. The best resolved are those at 850–830, 795–760 and 530–400 cm^{-1} with the first two best suited for enthalpy determinations. The lowest frequency triplet has the best separated bands but the one at 406 cm^{-1} for the gauche-2 fundamental is very weak and very near the FT–IR interferometer spectral cut-off. Therefore, the first two set of triplets were used for the conformational stability determinations.

To determine the relative stability of all three conformers of epichlorohydrin in a liquid xenon solution, the variable temperature study has been carried out at eight different temperatures varying from −40 to −105°C. Two of the well-resolved conformer triplets are shown in Figs. 3 and 4. The features at 846, 852, and 838 cm^{-1} of the symmetric ring deformation and 794, 769 and 788 cm^{-1} of the other ring deformation have been assigned to the most stable gauche-2, the second most stable gauche-1, and high energy cis conformers, respectively. These

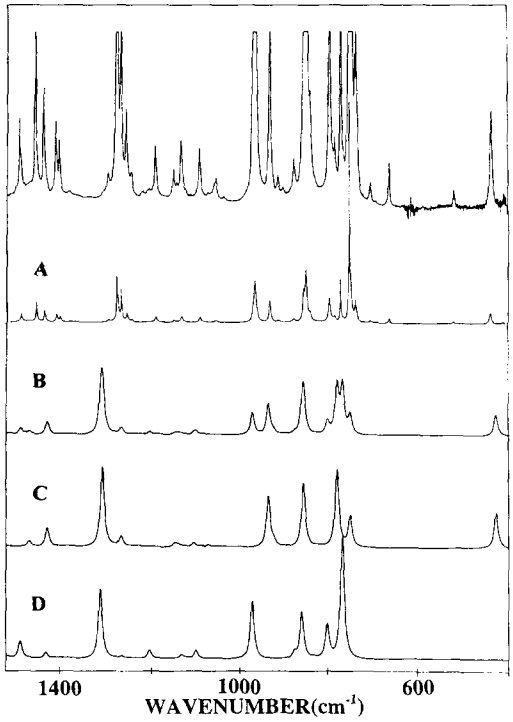

Fig. 2. Infrared spectra of epichlorohydrin dissolved in liquified xenon at −100°C in the region of (a) 1500–400 cm^{-1} with the top spectrum higher concentration; (b) mixture of gauche-1 and gauche-2; (c) pure gauche-1; and (d) pure gauche-2.

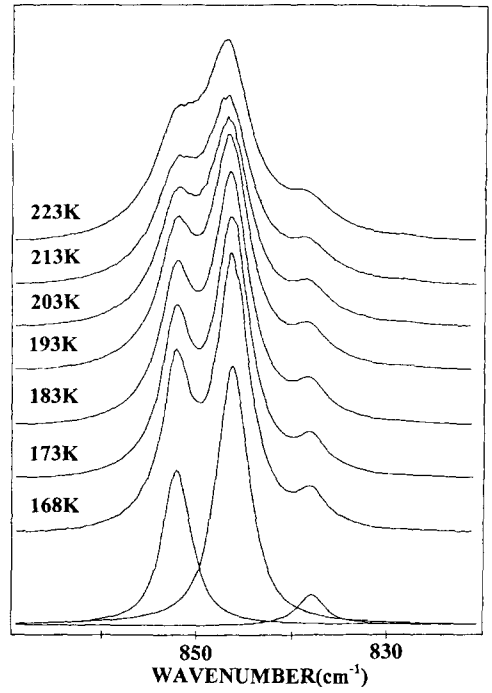

Fig. 3. Infrared spectra (870–820 cm^{-1}) for the variable temperature study of epichlorohydrin in a liquid xenon solution and the simulated profiles for 168 K at the bottom.

assignments are consistent with the predicted frequency order for the second set of triplets for these modes for the individual conformers from the ab initio calculations whereas for the higher frequency triplets the predicted order for the gauche-2 and gauche-1 bands are reversed. Also the weakest band in each triplet is assigned to the highest energy cis conformer. All of these experimental spectra have been least-squares fitted using a set of Gaussian–Lorentz sum profiles for obtaining reliable intensities and the resulting integrated intensities are summarized in Table 2. Using these values, van't Hoff plots have been made for each set of triplets (Fig. 5). The values for ΔH have been calculated to be 51 ± 14 cm^{-1} (145 ± 40 cal mol^{-1}) and 213 ± 97 cm^{-1} (608 ± 278 cal mol^{-1}) for the gauche-2 to gauche-1 and gauche-2 to cis forms, respectively. The latter value has a large statistical uncertainty because of the weakness of the bands for the cis conformer.

Even though previous studies [5,10] reported the enthalpy differences of the liquid, we have redetermined these values from the well resolved Raman lines of the ring–$C(Cl)H_2$ out-of-plane bend. Charles, et al. [10] determined the ΔH on the basis of the infrared intensities for the 960/925 cm^{-1} doublet. In this study, the line at 960 cm^{-1}, which they [10] assigned as a fundamental of gauche-2, has been found to not be a single band from one conformer but has a line from the cis conformer underneath it. Kalasinsky and Wurrey [5] also determined the ΔH values of the liquid to be 1.2 ± 0.2 and 0.7 ± 0.10 kcal mol^{-1} from the triplet at 735, 721 and 695 cm^{-1} (ν_{20}, C–Cl stretch) assigned to the cis, gauche-1 and gauche-2 conformers, respectively. In our study, this triplet has been assigned to the gauche-2, gauche-1 and cis conformers in the order of the 735, 721 and 691 cm^{-1} bands, respectively.

Therefore, we have carried out the variable temperature study of the Raman spectra of the liquid from 23 to −39°C for the clearly resolved triplet

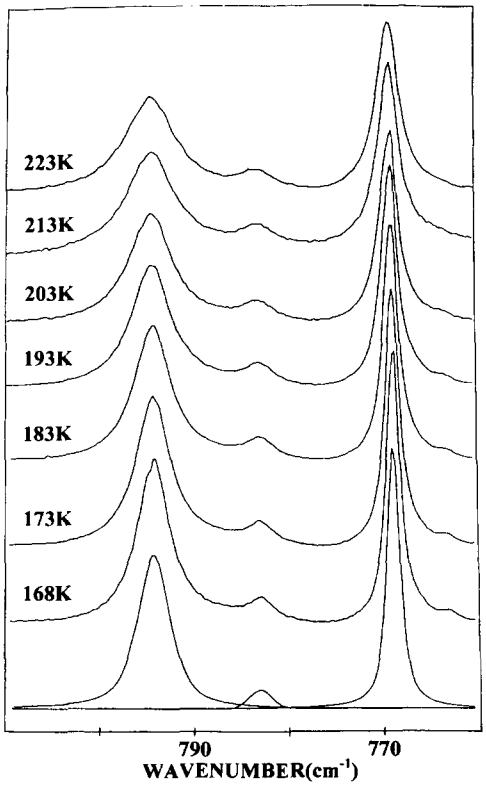

Fig. 4. Infrared spectra (810–760 cm^{-1}) for the variable temperature study of epichlorohydrin in a liquid xenon solution and the simulated profiles for 168 K at the bottom.

of the ring–$C(Cl)H_2$ out-of-plane bending mode. The resulting intensities are summarized in Table 3 and a van't Hoff plot is shown in Fig. 6. The corresponding values for ΔH have been obtained to be 383 ± 28 cm^{-1} (1.09 ± 0.08 kcal mol^{-1}) and 358 ± 12 cm^{-1} (1.02 ± 0.03 kcal mol^{-1}) for the gauche-1 to gauche-2 and gauche-1 to cis conformers, respectively. From these results, we have concluded that the most stable rotamer in the liquid is the polar gauche-1 rotamer and the other polar form of cis is slightly more stable than the least polar gauche-2 form.

4. Ab initio calculations

In order to provide additional information with regard to the structure and form of the normal vibrational modes of epichlorohydrin, we have carried out LCAO-MO-SCF restricted Hartree–Fock calculations. These calculations have been performed with the Gaussian-92 program [14] using the 3-21G* and 6-31G* basis sets with gaussian functions at the restricted Hartree–Fock (RHF) level and with full electron correlation [15] to the second order (MP2) for obtaining the optimized geometries and ab initio frequencies for the gauche-2, gauche-1, and cis conformations. The energy minima with respect to the

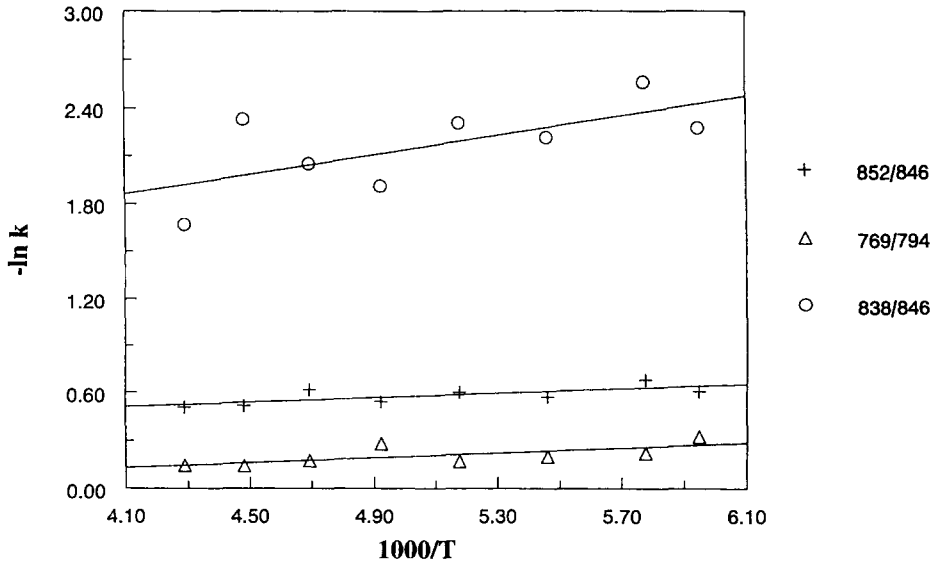

Fig. 5. A van't Hoff plot for epichlorohydrin dissolved in liquified xenon.

Table 2
Temperature and integrated intensity ratios for the conformational study of epichlorohydrin in liquid xenon

Vib. No.	T(K)	$K_1 = I_{\text{gauche-1}}/I_{\text{gauche-2}}$ [a]	$K_2 = I_{\text{cis}}/I_{\text{gauche-2}}$ [b]	$-\ln(K_1)$	$-\ln(K_2)$
ν_{18}	168	0.545	0.103	0.606	2.28
	173	0.507	0.077	0.680	2.56
	183	0.568	0.109	0.570	2.22
	193	0.548	0.099	0.601	2.31
	203	0.582	0.148	0.541	1.91
	213	0.540	0.129	0.617	2.05
	223	0.598	0.097	0.515	2.33
	233	0.602	0.188	0.507	1.67
ΔH[c]				48 ± 18 cm^{-1}	213 ± 97 cm^{-1}
ν_{19}	168	0.724		0.323	
	173	0.802		0.221	
	183	0.819		0.199	
	193	0.844		0.169	
	203	0.756		0.280	
	213	0.840		0.174	
	223	0.868		0.141	
	233	0.865		0.145	
ΔH[c]				53 ± 22 cm^{-1}	

[a] K_1 represents the ratios of the intensities of the 852/846 cm^{-1} for the ν_{18} and the intensities of the 769/794 cm^{-1} for the ν_{19}.
[b] K_2 represents the ratios of the intensities of the 838/846 cm^{-1}.
[c] Average value of ΔH is 51 ± 14 cm^{-1} (146 ± 40 cal mol^{-1}).

nuclear coordinates have been obtained by the simultaneous relaxation of all the geometric parameters using the gradient method of Pulay. [16,17] The calculated parameters are given in Table 4 for the gauche-2, gauche-1 and cis conformations. From Table 4, the structure which has the chlorine atom in the gauche-2 position (Fig. 1) relative to the ring is shown to be the thermodynamically preferred conformation with all three basis sets. The calculated torsional angles of the Cl atom to the ring for the gauche-2, gauche-1 and cis conformations are 117.4°, 117.3° and 2.5°, respectively. These results also give the C_2–C_3 distances and dipole moments of 1.501, 1.497 and 1.507 Å and 0.691, 3.893 and 3.267 D for the gauche-2, gauche-1, and cis conformers from the MP2/6-31G* calculations, respectively.

For the normal coordinate analysis, the following procedure has been used to transform ab initio results into the form required for our iterative normal coordinate programs. The Cartesian coordinates obtained for the optimized structure were input into the G-matrix program together with the complete set of thirty internal coordinates (Table 5 and Fig. 7). This complete set of internal coordinates has been used to form the symmetry coordinates and they are listed in Table 6. The output of this G-matrix program

Table 3
Temperature and integrated intensity ratios for the conformational study of epichlorohydrin in the liquid phase

T(K°)	$K_1 = I_{\text{gauche-2}}/I_{\text{gauche-1}}$ [a]	$K_2 = I_{\text{cis}}/I_{\text{gauche-1}}$ [b]	$-\ln(K_1)$	$-\ln(K_2)$
234	0.2516	0.2089	1.380	1.566
240	0.2664	0.2298	1.323	1.479
251	0.3046	0.2494	1.189	1.389
260	0.3159	0.2663	1.152	1.323
267	0.3222	0.2835	1.133	1.261
278	0.3552	0.3015	1.035	1.199
296	0.4254	0.3343	0.855	1.096

[a] K_1 represents the ratios of the Raman line intensities of the 413/443 cm^{-1}.
[b] K_2 represents the ratios of the Raman line intensities of the 517/443 cm^{-1}.

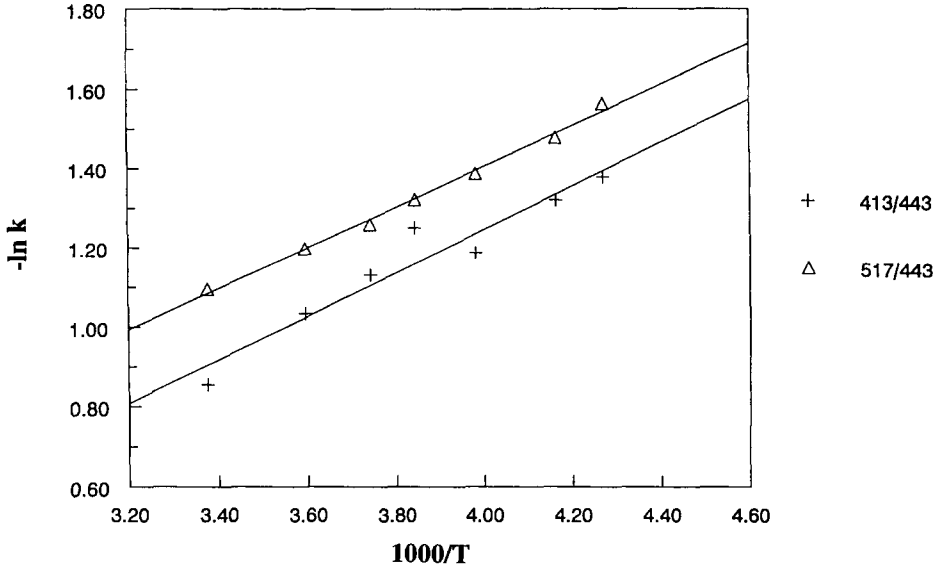

Fig. 6. A van't Hoff plot for liquid epichlorohydrin using the intensities of the Raman triplet line of the ring–$C(Cl)H_2$ out-of-plane bend.

consists of the B-matrix and the unsymmetrized G-matrix. The B-matrix has been used to convert the ab initio force field in Cartesian coordinates to a force field in the desired internal coordinates for the gauche-2, gauche-1 and cis conformers which can be obtained from the authors. All diagonal elements of the obtained force fields in internal coordinates have been assigned scaling factors. The force field has then been input, along with the unsymmetrized G-matrix and scaling factors, into the perturbation program written by Schachtschneider [18]. Initially, all scaling factors have been kept fixed at a value of 1.0 to produce the pure ab initio calculated vibrational frequencies and the potential energy distributions (P.E.D.) which are given in Table 7. Subsequently, a scaling factor of 0.9 for all coordinates except 1.0 for the torsion has been utilized to obtain the scaled frequencies. The resultant frequencies from the scaled force field are also listed in Table 7.

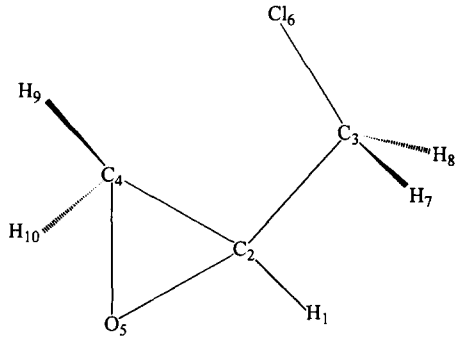

Fig. 7. Geometrical model for epichlorohydrin in the cis conformation.

5. Vibrational assignment

The infrared spectrum of the xenon solution and the ab initio calculations indicate that many normal modes should be reassigned from those given earlier [5] since they were assigned based on the gauche-1 form as the most stable conformation in the gas and liquid phases. On the basis of the scaled ab initio frequencies along with calculated infrared intensities and the principle that the two polar forms can be stabilized in the liquid phase and the gauche-1 is the only conformer in the solid, we have reassigned many of the fundamentals for each of the conformers. Our observations of the FT–IR spectrum of the xenon solution with the relatively sharp bands aided the assignment of the individual bands to the gauche-2 and gauche-1 conformers. In this investigation, we have concluded that both the more polar gauche-1 and cis forms become more abundant in the liquid phase whereas the bands of the less polar gauche-2 form becomes less intense than the corresponding

Table 4
Structural parameters, dipole moments, rotational constants and energies of epichlorohydrin[a]

Parameter	RHF/3-21G*			RHF/6-31G*			MP2/6-31G*			Microwave[b]		
	gauche-II	gauche-I	cis	gauche-II	gauche-I	cis	gauche-II	gauche-I	cis	gauche-II	gauche-I	cis
$r(C_2-C_3)$	1.499	1.496	1.505	1.504	1.501	1.508	1.501	1.497	1.507	1.522	1.513*	1.522
$r(Cl-C_3)$	1.813	1.810	1.801	1.793	1.793	1.786	1.787	1.787	1.779	1.767	1.760	1.794
$r(C_2-C_4)$	1.469	1.475	1.470	1.451	1.455	1.452	1.463	1.467	1.463	1.471*	1.471*	1.471*
$r(C_2-O)$	1.468	1.464	1.459	1.400	1.397	1.393	1.439	1.435	1.431	1.436*	1.436*	1.436*
$r(C_4-O)$	1.476	1.473	1.477	1.407	1.403	1.407	1.445	1.442	1.447	1.436*	1.436*	1.436*
$r(H_1-C_2)$	1.071	1.071	1.074	1.077	1.077	1.081	1.090	1.090	1.093	1.082*	1.082*	1.082*
$r(H_7-C_3)$	1.077	1.077	1.078	1.079	1.078	1.080	1.091	1.091	1.093	1.092*	1.092*	1.092*
$r(H_8-C_3)$	1.076	1.077	1.078	1.078	1.080	1.080	1.091	1.092	1.092	1.092*	1.092*	1.092*
$r(H_9-C_4)$	1.071	1.071	1.069	1.077	1.077	1.074	1.088	1.088	1.086	1.082*	1.082*	1.082*
$r(H_{10}-C_4)$	1.070	1.071	1.071	1.076	1.076	1.077	1.087	1.088	1.088	1.082*	1.082*	1.082*
$<(C_3-C_2-H_1)$	116.6	116.6	113.0	115.2	115.2	111.2	115.8	115.7	112.0			
$<(Cl-C_3-C_2)$	109.8	110.9	113.5	110.5	111.4	114.7	110.1	111.0	113.8	110.97	109.45*	110.94
$<(C_4-C_2-C_3)$	119.4	118.9	123.6	121.5	120.6	125.9	46.5	46.2	51.9			
$<(O-C_2-C_3)$	112.6	114.4	116.9	114.3	116.4	118.3	154.8	144.8	151.6			
$<(C_4C_2O)$	60.4	60.1	60.6	59.1	58.9	59.3	108.3	98.6	99.7			
$<(C_2OC_4)$	59.8	60.3	60.1	62.2	58.6	62.4	67.7	76.8	75.6			
$<(H_7-C_3-C_2)$	111.8	110.3	110.2	111.1	110.7	109.8	111.3	109.8	109.5	109.45*	109.45*	109.45*
$<(H_8-C_3-C_2)$	110.7	111.4	110.0	111.0	111.0	109.6	110.0	111.0	109.6	109.45*	109.45*	109.45*
$<(H_9-C_4-C_2)$	119.1	119.4	119.5	119.9	120.1	120.3	119.1	119.7	119.6			
$<(H_{10}-C_4C_2)$	119.3	119.2	118.8	119.8	119.7	119.2	119.8	119.5	119.3			
$<(H_9C_4H_{10})$	116.4	116.2	116.8	115.4	115.2	115.8	115.7	115.6	116.2			
$\tau(Cl-C_3-C_2-H_1)$	− 65.5	53.0	180.2	− 60.7	55.4	185.3	− 62.6	57.3	182.5	− 70.21	54.02	173.22
$\tau(C_4-C_2-C_3-H_1)$	155.9	154.1	153.5	156.2	153.8	154.2						
$\tau(O-C_2-C_3-H_1)$	− 136.4	− 137.9	− 135.5	− 136.4	− 138.3	− 134.9						
$\tau(H_7-C_3-C_2-Cl)$	118.4	118.0	120.1	118.6	119.0	120.5	112.8	111.4	111.6			
$\tau(H_8-C_3-C_2-Cl)$	− 118.8	− 118.6	− 118.9	− 119.5	− 118.7	− 119.8	111.6	112.5	111.5			
$\tau(H_9-C_4-C_2-O)$	− 103.4	− 103.0	− 102.5	− 103.0	− 102.8	− 102.5	− 103.6	−103.1	− 102.8			
$\tau(H_{10}-C_4-C_2-O)$	103.0	103.4	102.9	103.0	103.3	103.0	103.2	103.7	103.2			
μ_a	0.465	2.009	0.945	0.119	2.022	0.962	− 0.074	0.753	− 2.447			
μ_b	0.572	3.135	2.429	0.771	3.584	1.955	0.651	3.260	1.997			
μ_c	0.128	0.506	2.570	0.092	0.593	2.222	− 0.218	− 1.989	− 0.838			
μ_t	0.749	3.758	3.660	0.785	4.158	3.112	0.691	3.893	3.267			
A	12813	13187	8533	13571	13879	9081	13171	13268	8785	12739	13377	8379
B	2014	2034	2645	2003	2054	2590	2024	2090	2655	2067	2082	2841
C	1867	1892	2390	1871	1917	2340	1884	1938	2397	1881	1932	2511
$-(E+647)$	0.648731	0.646746	0.644824	3.809604	3.808316	3.806241	4.504574	4.503673	4.502119			
ΔE (cm^{-1})	0	436	857	0	283	738	0	198	539			

[a]Bond lengths in Å, bond angles in degree, dipole moments in Debye, total energy in Hartrees, and rotational constants in MHz.
[b]Taken from Ref. [3,4]. The parameters denoted with an asterisk (*) were held fixed at the given values during the fit.

Table 5
Internal coordinate definitions[a] for epichlorohydrin

Coordinate Involved	Definition	Coordinate Involved	Definition
C_2O stretch	X	OC_2H bend	ϕ
C_4O stretch	R	C_4C_2H bend	λ
C_2C_4 stretch	D	C_3C_2H bend	ω
C_2C_3 stretch	Q	OC_4H_9 bend	σ
C_2H stretch	P	$C_2C_4H_9$ bend	ϵ
C_4H_9 stretch	Z_1	OC_4H_{10} bend	η
C_4H_{10} stretch	Z_2	$C_2C_4H_{10}$ bend	ψ
C_3Cl stretch	T	HC_4H bend	χ
C_3H_7 stretch	Y_1	C_2C_3Cl bend	θ
C_3H_8 stretch	Y_2	$C_2C_3H_7$ bend	μ_1
C_2OC_4 bend	α	$C_2C_3H_8$ bend	μ_2
OC_2C_4 bend	β	ClC_3H_7 bend	ρ_1
OC_4C_2 bend	δ	ClC_3H_8 bend	ρ_2
OC_2C_3 bend	γ	HC_3H bend	Δ
$C_4C_2C_3$ bend	π	asymmetric torsion	τ

[a]For atom denotation see Fig. 7.

bands in the vapor. This conclusion is consistent with that of Charles, et al. [10]. Therefore, the bands of polar conformers will be weaker or disappear in the spectrum of the vapor or xenon solution and become stronger or appear in the liquid with the bands of the gauche-1 the only ones in the solid.

With these points we have carefully reassigned the fundamentals of all three conformers and most

Table 6
Symmetry coordinates for epichlorohydrin

Species	Description	Symmetry coordinate
A	*CH_2 antisymmetric stretch	$S_1 = Z_1 - Z_2$
	CH_2 antisymmetric stretch	$S_2 = Y_1 - Y_2$
	α-CH stretch	$S_3 = P$
	*CH_2 symmetric stretch	$S_4 = Z_1 + Z_2$
	CH_2 symmetric stretch	$S_5 = Y_1 + Y_2$
	*CH_2 deformation	$S_6 = 4\chi - \sigma - \epsilon - \eta - \psi$
	CH_2 deformation	$S_7 = \Delta$
	ring breathing	$S_8 = X + R + D$
	CH_2 rock	$S_9 = \mu_1 + \mu_2 - \rho_1 - \rho_2$
	C–H in-plane bend	$S_{10} = 2\omega - \phi - \lambda$
	CH_2 wag	$S_{11} = \mu_1 - \mu_2$
	C–H out-of-plane bend	$S_{12} = \phi - \lambda$
	*CH_2 wag	$S_{13} = \sigma - \epsilon + \eta - \psi$
	CH_2 twist	$S_{14} = \rho_1 - \rho_2$
	8CH_2 rock	$S_{15} = \sigma + \epsilon - \eta - \psi$
	C–C stretch	$S_{16} = Q$
	*CH_2 twist	$S_{17} = \sigma - \epsilon - \eta + \psi$
	ring symmetric deformation	$S_{18} = 2\alpha - \beta - \delta$
	ring antisymmetric deformation	$S_{19} = X - R$
	C–Cl stretch	$S_{20} = T$
	ring $-C(Cl)H_2$ out-of-plane bend	$S_{21} = \pi - \gamma$
	ring $-C(Cl)H_2$ in-plane bend	$S_{22} = \pi + \gamma$
	CCCl bend	$S_{23} = \theta$
	$-C(Cl)H_2$ asymmetric torsion	$S_{24} = \tau$

*Ring modes.

Table 7
Observed and calculated frequencies (cm^{-1}) and potential energy distribution (P.E.D.) for epichlorohydrin

Vib.		*gauche*-2					*gauche*-1					*cis*				
No.	Fundamental[a]	Ab Initio[b]	Fixed Scaled[c]	IR Int.[d]	Obs.[e]	P.E.D.	Ab Initio[b]	Fixed Scaled[c]	IR Int.[d]	Obs.[e]	P.E.D.	Ab Initio[b]	Fixed Scaled[c]	IR Int.[d]	Obs.[e]	P.E.D.
ν_1	*CH_2 antisymmetric stretch	3275	3107	16.9	3063	$99S_1$	3270	3102	18.0	3056	$99S_1$	3289	3120	10.3	3068	$97S_1$
ν_2	CH_2 antisymmetric stretch	3230	3064	5.6	3024	$94S_2$	3224	3059	5.4	3016*	$93S_2$	3209	3044	3.8		$37S_2,61S_3$
ν_3	C-H stretch	3203	3038	8.0	3008	$93S_3$	3199	3035	8.0	3015	$93S_3$	3185	3021	15.9	(2991)	$99S_3$
ν_4	*CH_2 symmetric stretch	3175	3012	12.9	2975	$99S_4$	3171	3009	15.5	2963	$99S_4$	3164	3002	24.8		$36S_4,61S_2$
ν_5	CH_2 symmetric stretch	3158	2996	9.5	2940	$100S_5$	3150	2988	11.7	2936	$99S_5$	3143	2982	7.3		$98S_5$
ν_6	*CH_2 deformation	1583	1502	1.3	1490	$80S_6$	1582	1500	0.7	1487	$82S_6,11S_8$	1581	1500	4.5		$84S_6$
ν_7	CH_2 deformation	1548	1469	7.2	1456	$87S_7,12S_8$	1528	1450	2.3	1437	$96S_7$	1535	1456	4.9		$94S_7$
ν_8	ring breathing	1489	1413	2.5	1412	$18S_8,37S_{10},18S_6$	1316	1249	4.3	1253	$41S_8,31S_{10}$	1482	1406	11.5	1402	$42S_8,17S_{22},12S_9,11S_{11}$
ν_9	CH_2 rock	1364	1294	28.5	1275	$83S_9$	1360	1290	32.8	1267	$81S_9,12S_{10}$	1389	1317	17.0	(1292)	$69S_9$
ν_{10}	C-H bend	1316	1248	1.1	1246	$50S_{10},27S_8$	1486	1410	7.7	1405	$40S_{10},18S_8,14S_6$	1332	1264	3.0	1256	$71S_{10}$
ν_{11}	CH_2 wag	1251	1187	3.6	1186	$38S_{11},19S_{14},14S_{16}$	1276	1211	0.7	(1207)	$35S_{11},32S_{14}$	1274	1208	0.7	(1202)	$44S_{11},17S_{10}$
ν_{12}	C-H bend	1200	1138	0.5	1151	$48S_{12},33S_{15}$	1192	1131	1.6	(1142)	$41S_{12},23S_{15},18S_{13}$	1189	1128	0.4		$86S_{12}$
ν_{13}	*CH_2 wag	1177	1116	1.8	1134	$88S_{13}$	1183	1123	1.1	1139*	$51S_{13},20S_{15}$	1183	1122	2.3		$55S_{13},31S_{15}$
ν_{14}	CH_2 twist	1143	1085	3.5	1092	$22S_{14},26S_{17},17S_{16},16S_{15}$	1149	1090	1.8	1091*	$23S_{14},21S_{16},19S_{13},14S_{17}$	1120	1062	1.3	1073	$72S_{14},10S_{15}$
ν_{15}	*CH_2 rock	1107	1050	0.03	(1053)	$30S_{15},32S_{12},22S_{14}$	1115	1058	1.1	1055	$36S_{15},27S_{12},24S_{17}$	1083	1028	2.2	(1034)	$41S_{15},22S_{13},11S_{16}$
ν_{16}	C-C stretch	1013	961	23.9	964	$20S_{16},18S_{17},17S_{18},16S_8,13S_{14}$	977	926	20.7	934	$17S_{16},26S_{19},19S_{11},17S_{14}$	1019	967	23.2	972	$66S_{16},20S_{17},12S_{11},10S_{19}$
ν_{17}	*CH_2 twist	916	869	2.6	(875)	$32S_{17},32S_{11}$	964	914	2.0	(911)	$24S_{17},34S_{18},11S_{11}$	951	902	2.1		$19S_{17},28S_{19},21S_{16}$
ν_{18}	ring symmetric deformation	898	852	19.2	842	$38S_{18},40S_{19}$	895	849	26.3	853	$43S_{18},18S_{17}$	885	840	30.0	(838)	$59S_{18},16S_{19},15S_{16}$
ν_{19}	ring antisymmetric deformation	839	797	13.6	794	$49S_{19},28S_{18}$	818	776	32.0	775	$60S_{19},23S_{20}$	833	791	14.8	788	$26S_{19},20S_{20},10S_{17}$
ν_{20}	C-Cl stretch	805	764	50.4	755	$79S_{20}$	788	747	12.4	743	$52S_{20},12S_{23},10S_{19}$	742	704	11.8	(703)	$43S_{20},20S_{23},12S_{17},11S_{19}$
ν_{21}	ring -C(Cl)H_2 out-of-plane bend	425	403	0.2	406	$47S_{21},16S_{23}$	450	427	14.5	438	$36S_{21},21S_{22},19S_{23}$	542	515	9.7	521	$30S_{21},33S_{20},20S_{23}$
ν_{22}	ring -C(Cl)H_2 in-plane bend	382	362	4.3	371	$67S_{22},12S_{20}$	379	360	1.2	371	$58S_{22},12S_{20}$	359	340	8.6		$77S_{22},10S_{16}$
ν_{23}	CCCl bend	216	205	12.8	214	$60S_{23},26S_{21}$	214	203	0.1	380*	$53S_{23},32S_{21},12S_{11}$	217	206	0.4		$54S_{23},22S_{22},11S_8$
ν_{24}	C(Cl)H_2 asymmetric torsion	96	90	7.5	90	$87S_{24},10S_{21}$	101	95	1.2	68*	$83S_{24}$	116	110	4.2		$81S_{24}$

[a]Asterisks (*) denote ring modes.

[b]Obtained from the MP2/6-31G* calculation.

[c]Scaled ab initio calculations with scaling factor of 0.9 for all coordinates except for the torsion.

[d]Calculated infrared intensities in km mol^{-1}.

[e]Frequencies are taken from the infrared or Raman spectra of the gas except those in parentheses which were taken from the infrared spectrum of the xenon solution, and those with an asterisk (*) from the Raman spectrum of the solid.

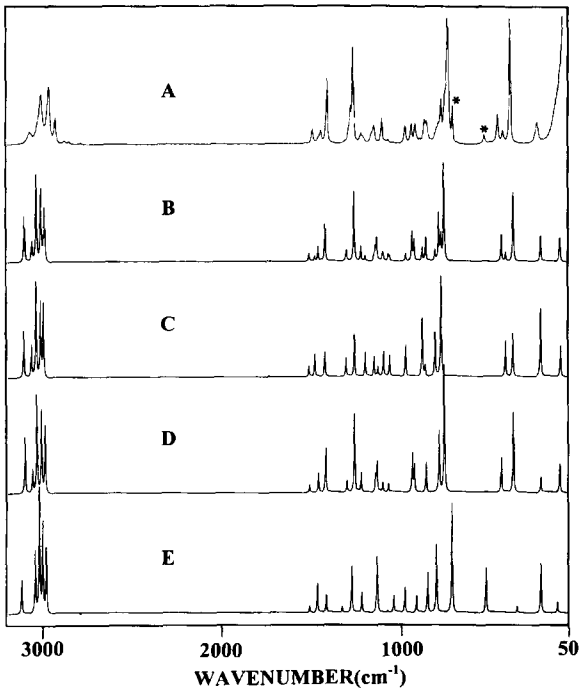

Fig. 8. Calculated Raman spectra (scattering activities from RHF/6-31G*) of (a) experimental of the liquid, with lines marked with asterisks due to the cis conformer; (b) mixture of the gauche-1 and gauche-2 conformers; (c) pure gauche-2; (d) pure gauche-1; and (e) pure cis epichlorohydrin.

of those which were previously [5] assigned to the gauche-1 conformer switched to those for the gauche-2 form and vice versa. The bands at 1253 and 1405 cm^{-1} in the infrared spectrum of the gas have been assigned as the ring breathing and C_2–H in-plane bend of the gauche-1 form, respectively, which are consistent with the calculated potential energy distribution listed in Table 7. The bands at 853 and 842 cm^{-1} in the infrared spectrum of the gas, which were assigned as the two different fundamentals [5], ν_{17} and ν_{18}, have now been assigned as the same symmetric ring deformation of the gauche-1 and gauche-2 conformer, respectively. Another major change has been for the ν_{21} mode. Previously ν_{22} had been assigned at 406 cm^{-1} in the Raman spectrum of the gas but we have reassigned it to the ν_{21} fundamental of the gauche-2 form which is consistent with the scaled ab initio frequency for this fundamental. All of the vibrational assignments for the remaining fundamentals for all three conformers are summarized in Table 7.

6. Discussion

From the ab initio calculations, the gauche-2 conformer is shown to be thermodynamically preferred in all three calculations (Table 4). The infrared spectrum of the xenon solution also shows that the gauche-2 conformer is the most stable conformer and the gauche-1 the second most stable form in this non-polar solvent. These results should also reflect the stability in the gas phase since xenon should have a relatively small effect on the conformer stability [12] as was found for n-butane. Although the calculated energy differences between the gauche-2 and gauche-1 forms is relatively small (198 cm^{-1} from the MP2/6-31G* calculation), it is doubtful that the order of stability would change with larger basis sets. Therefore, both the ab initio calculations and the spectral data from the xenon solution indicate that the gauche-2 conformer is the most stable rotamer and that the gauche-2 conformer is undoubtedly the most stable rotamer in the isolated vapor state [12,20].

From the Raman spectrum of the liquid, it has been concluded that the polar gauche-1 and cis forms become more stable in the condensed state. Therefore, the gauche-1 rotamer of epichlorohydrin becomes predominant in the liquid phase and the only form in the solid. Even though the orientation of the gauche-2 form is much more favored than the cis on the basis of steric arguments, it has been determined that the cis form is slightly more stable than the gauche-2 rotamer in the liquid state. These polar forms may be stabilized by hydrogen bonding in the condensed phases but the gauche-2 form is sterically favored in the isolated state.

Raman (Fig. 8) and infrared (Fig. 2) spectra for epichlorohydrin were calculated using the frequencies and intensities determined from the MP2/6-31G* calculations and scattering activities from the RHF/6-31G* calculations. The Gaussian-92 program [14] with the option of calculating the polarizability derivatives was used. The Raman scattering cross sections, $\partial\sigma_j/\partial\Omega$ which are proportional to the Raman intensities, can be calculated from the scattering activities and the predicted frequencies for each

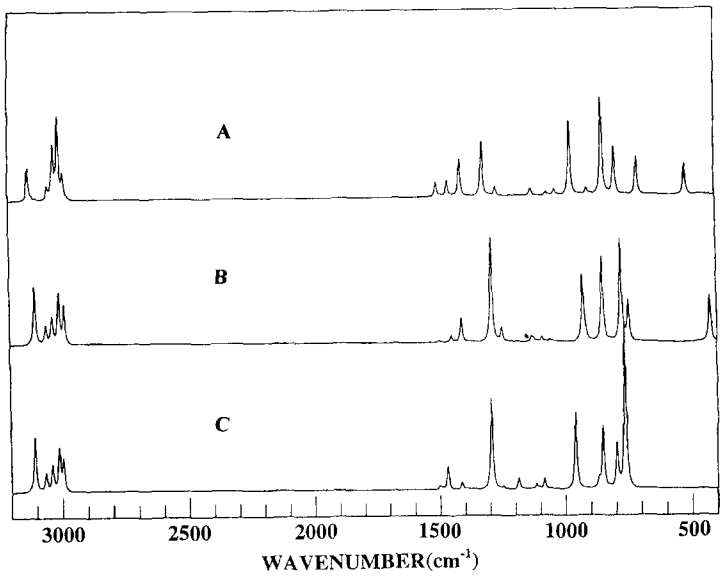

Fig. 9. Calculated (MP2/6-31G*) infrared absorbance spectra of (a) cis; (b) gauche-1; and (c) gauche-2 epichlorohydrin.

normal mode using the relationship [19]:

$$\frac{\partial\sigma_j}{\partial\Omega}=\left(\frac{2^4\pi^4}{45}\right)\left(\frac{(\nu_0-\nu_j)^4}{1-\exp\left[-\frac{hc\nu_j}{kT}\right]}\right)\left(\frac{h}{8\pi^2c\nu_j}\right)S_j$$

where ν_0 is the exciting frequency, ν_j is the vibrational frequency of the jth normal mode, and S_j is the corresponding Raman scattering activity. To obtain the polarized Raman scattering cross sections, the polarizabilities are incorporated into S_j by $S_j[(1 - r_j)/(1 + r_j)]$ where r_j is the depolarization ratio of the jth normal mode. The Raman scattering cross sections (RHF/6-311G*) and calculated frequencies (MP2/6-31G*) were used together with a Lorentzian line shape function to obtain the calculated spectra. Since the calculated frequencies are approximately 10% higher than those observed, the frequency axis of the theoretical spectrum was compressed by a factor of 0.9. The predicted Raman spectrum of each of the conformers is shown in Fig. 8. Additionally, the mixture of the two most abundant conformers with the experimental ΔH of 383 cm^{-1} with the gauche-2 the more stable conformer is shown in Fig. 8(b). This spectrum should be compared to the experimental one shown in Fig. 8(a). The calculated spectrum has some small differences from the experimental spectrum, especially in the relative intensities of the bands in the 1100 cm^{-1} region. Nevertheless, it provides support for the assignment of the observed bands to the indicated fundamentals and the conclusions on the conformer stabilities. In Fig. 8(a) we have indicated the two clearly observed Raman lines of the cis conformer with asterisks and the higher frequency line is predicted to be one of the strongest lines in the Raman spectrum of the cis conformer (Fig. 8(e)). Thus the relative intensities of the two lines due to the cis conformer appear consistent with its abundance relative to the other two conformers.

Infrared intensities were also calculated based on the dipole moment derivatives with respect to the Cartesian coordinates. The derivatives were taken from the ab initio calculations (MP2/6-31G*) transformed to normal coordinates by:

$$\left(\frac{\partial\mu u}{\partial Q_i}\right)-\sum_j\left(\frac{\partial\mu u}{\partial X_j}\right)L_{ji}$$

where Q_i is the ith normal coordinate, X_j is the jth Cartesian displacement coordinate, and L_{ji} is the transformation matrix between the Cartesian

displacement coordinates and normal coordinates. The infrared intensities were then calculated by:

$$I_i = \frac{N\pi}{3c^2}\left[\left(\frac{\partial\mu u_x}{\partial Q_i}\right)^2 + \left(\frac{\partial\mu u_y}{\partial Q_i}\right)^2 + \left(\frac{\partial\mu u_x}{\partial Q_i}\right)^2\right]$$

The predicted infrared spectra of the gauche-2, gauche-1 and cis conformers are shown in Fig. 9(c), 9(b) and 9(a), respectively. The mixture of the two most abundant conformers with the experimental ΔH of 51 cm^{-1} with the gauche-2 conformer the more stable rotamer is shown in Fig. 2(b). Again, the frequency axis of the theoretical spectrum was shifted by a factor of 0.9. The infrared spectrum of the sample dissolved in xenon is shown in Fig. 2(a). The bands at 788, 703 and 520 cm^{-1} are due to fundamentals of the cis conformer but excluding these bands there is rather good agreement with the observed spectrum of the sample dissolved in xenon (Fig. 2(a)). There are some intensity differences in the 770–795 cm^{-1} region but the antisymmetric deformation of the two conformers are badly overlapped in the infrared spectrum of the sample dissolved in xenon whereas they are well resolved in the calculated spectrum (Fig. 2(b)). The predicted spectrum clearly shows the utility of the calculated infrared intensities for supporting the vibrational assignments and how bands can be assigned to the individual conformers.

In conclusion, three conformers of epichlorohydrin have been clearly identified in the FT–IR spectrum of the xenon solution as well as in the Raman spectrum of the liquid and the enthalpy differences determined. With these results, the fundamental frequencies have been reassigned for all three conformers. Finally, it should be mentioned that the theoretical ab initio calculation and noble gas isolation techniques [12] are powerful tools for analyzing the complex conformational stabilities of the three stable rotamers along with their vibrational assignments.

Acknowledgements

JRD would like to acknowledge partial support of these studies by the University of Missouri-Kansas City Faculty Research Grant program.

References

[1] M.J. Shapiro, J. Org. Chem. 42 (1977) 1434.
[2] F.G. Fujiwara, J.C. Chang, H. Kim, J. Mol. Struct. 41 (1977) 177.
[3] M.A. Mohammadi, W.V.F. Brooks, J. Mol. Spectrosc. 73 (1978) 353.
[4] M.A. Mohammadi, W.V.F. Brooks, J. Mol. Spectrosc. 78 (1979) 89.
[5] V.F. Kalasinsky, C.J. Wurrey, J. Raman Spectrosc. 9 (1980) 315.
[6] M.J. Aroney, K.E. Calderbank, H.J. Stootman, Aust. J. Chem. 31 (1978) 2303.
[7] M. Hayashi, K. Hamo, K. Ohno, H. Murata, Bull. Chem. Soc. Jpn. 45 (1972) 949.
[8] L. Paolini, M. Landi-Vittory, Sci. Rep. 1st Super Sanita 2 (1962) 37.
[9] O. Ballans, J. Wagner, Z. Phys. Chem. (Leipzig) 45 (1940) 272.
[10] S.W. Charles, G.I.L. Jones, N.L. Owen, J. Mol. Struct. 20 (1974) 83.
[11] Q. Shen, J. Mol. Struct. 130 (1985) 275.
[12] W.A. Herrebout, B.J. van der Veken, A. Wang, J.R. Durig, J. Phys. Chem. 99 (1995) 578.
[13] F.A. Miller, B.M. Harney, Appl. Spectrosc. 24 (1970) 291.
[14] Gaussian-92/DFT, Revision G.3, M.J. Frisch, G.W. Trucks, H.B. Schlegel, P.M.W. Gill, B.G. Johnson, M.W. Wong, J.B. Foresman, M.A. Robb, M. Head-Gordon, E.S. Replogle, R. Gomperts, J.L. Andres, K. Raghavachari, J.S. Binkley, C. Gonzalez, R.L. Martin, D.J. Fox, D.J. DeFrees, J. Baker, J.J.P. Stewart, J.A. Pople, Gaussian, Inc., Pittsburgh, PA, 1993.
[15] C. Moller, H.S. Plesset, Phys. Rev. 46 (1934) 618.
[16] G. Fogorasi, P. Pulay, in: J.R. Durig (Ed.), Vibrational Spectra and Structure, Vol. 14, Elsevier, Amsterdam, 1985.
[17] P. Pulay, Mol. Phys. 17 (1969) 197.
[18] J. H. Schachtschneider, Vibrational Analysis of Polyatomic Molecules, Parts V and VI, Technical Report Nos. 231 and 57, Shell Development Co., Houston, TX, 1964 and 1965.
[19] G. W. Chantry, in A. Anderson (Ed.), The Raman Effect, Vol. 1, Chap. 2 Marcel Dekker Inc., New York, 1971.
[20] W.A. Herrebout, B.J. van der Veken, J. Phys. Chem. 100 (1996) 9671.